

Discrepancies between global reanalyses and observations in the interdecadal variations of Southeast Asian cold surge

Wan-Ru Huang,^{a*} Shih-Yu Wang^b and Johnny C. L. Chan^a

^a Guy Carpenter Asia-Pacific Climate Impact Centre, School of Energy and Environment, City University of Hong Kong, Hong Kong, China

^b Utah Climate Center, Utah State University, Logan, UT, USA

ABSTRACT: The Siberian High (SH) is an important part of the East Asian winter monsoon (EAWM) and is closely linked to cold surges. Previous studies revealed a pronounced decline in the strength of the SH during the late 20th century accompanied with a coherent decrease in the frequency of cold surges. However, studies using different data sets yielded different behaviour of the trends. Here we examine the interdecadal variations of the SH and cold surges deduced from six modern global reanalysis data sets. Discrepancies in such variations are found between the reanalysis data sets and observations as well as among different reanalysis data sets. Such discrepancies contribute to inconsistent interdecadal variations of the cold surge frequency in different reanalysis data sets. Potential causes of this situation are discussed. Copyright © 2010 Royal Meteorological Society

KEY WORDS Siberia High; cold surge; interdecadal variation; East Asian winter monsoon

Received 7 January 2010; Revised 3 August 2010; Accepted 31 August 2010

1. Introduction

The semi-permanent Siberian High (SH) spanning the Eurasian continent is a key element of the East Asian winter monsoon (EAWM; Figure 1(a)) that is linked to cold surges (Cheang, 1987; Lau and Chang, 1987; Chan and Li, 2004). The cold surge frequency varies coherently with the SH fluctuations on both the interannual and decadal time scales (Ding, 1990; Wu and Chan, 1997; Zhang *et al.*, 1997; Jeong and Ho, 2005). During the late 20th century, the SH underwent a drastic decrease in strength (Gong and Ho, 2002), as can be seen in the time series of observed sea-level pressure (SLP; Trenberth and Paolino, 1980) averaged over the SH (40° – 65° N, 80° – 120° E) (Figure 1(b)). The SH strength decreased most rapidly during the 1978–2001 period (Panagiotopoulos *et al.*, 2005). Recent studies (Hong *et al.*, 2008; Wu and Leung, 2008) found that this SH decline is likely linked to the interdecadal variation of the North Atlantic Oscillation and the associated large-scale circulation across Eurasia.

Global reanalysis data sets (herein reanalyses) have been an important resource of EAWM research (Sun and Sun, 1995; Shi, 1996; Chen *et al.*, 2001; Wu and Wang, 2002; Chen *et al.*, 2004; Jhun and Lee, 2004; Gao, 2007). Numerous studies have noted discrepancies between different reanalyses in the spatial–temporal distribution of rainfall (Lim and Ho, 2000; Sumant and Alfredo, 2006; Zhao and Fu, 2006), pressure (Smith *et al.*, 2001; Ponte and Dorandeu, 2003; Salstein *et al.*, 2008), and

temperature (Greatbatch and Rong, 2006; Chen *et al.*, 2008). Discrepancies in the multi-decadal variation of surface pressure between reanalyses and observations (Yang *et al.*, 2002; Inoue and Matsumoto, 2004) are of particular concern as cold surges are closely linked to the SH. As implied in Panagiotopoulos *et al.* (2005), the SH decline derived from the reanalyses is not as pronounced as that found in observations. Clearly, there is a possibility that the cold surge frequency depicted by the reanalyses may not agree with the observations and with each other. This possibility is examined herein.

Studies using different reanalyses and different criteria also yield inconsistent trends in the cold surge frequency. For instance, a gradual decrease in the cold surge frequency was noted during the time period of 1980–1990 (Zhang *et al.*, 1997) and 1979–2000 (Chen *et al.*, 2004), whereas a much stronger decrease during a similar time period was revealed in Hong *et al.* (2008) and Wu and Leung (2008). Currently, six reanalyses are available and have been used extensively in climate research. It is therefore important to examine if these reanalyses produce consistent variations of EAWM and the cold surge frequency. Such a study will provide a validation for future EAWM research using reanalyses. The six reanalyses are first introduced in Section 2. Results are then presented in Section 3, followed by a summary in Section 4.

2. Data and cold surge definition

The six reanalyses evaluated are introduced in Table I including their acronyms, available time period, model resolution, basic assimilation scheme, and references. Data of these reanalyses are all extracted from the National Center for Atmospheric Research Mass Storage

*Correspondence to: Wan-Ru Huang, Guy Carpenter Asia-Pacific Climate Impact Centre, School of Energy and Environment, City University of Hong Kong, Tat Chee Avenue, Kowloon, Hong Kong, China. E-mail: wrhuang@cityu.edu.hk

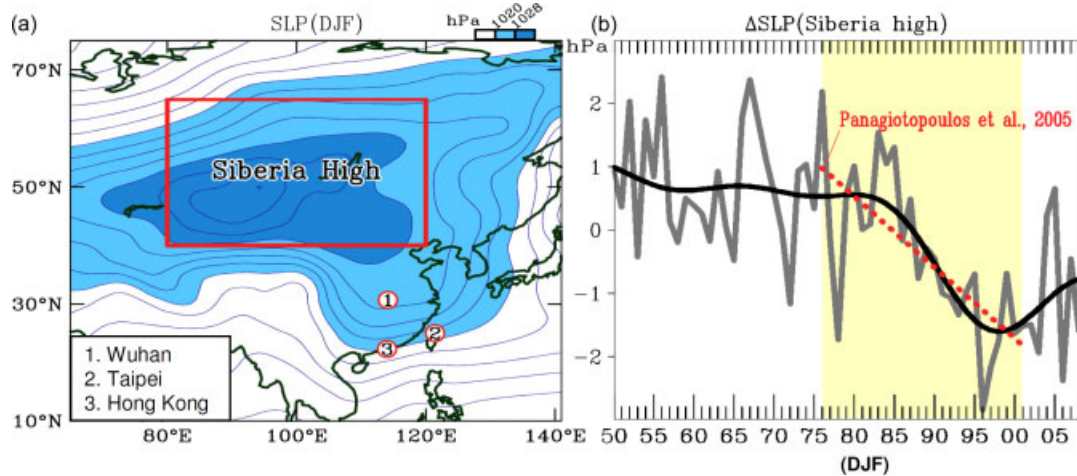


Figure 1. (a) The SLP for winter (December–February) climatology averaged over the 1979–2008 period derived from the ERA40/I reanalyses. Areas with SLP larger than 1020 and 1028 hPa are shaded (colour scale given in the top right). (b) Time series of the SLP anomalies (Δ SLP) averaged over the Siberia high [(80°–120°E, 40°–65°N) as outlined in (a)] from 1950 to 2008 using the Trenberth–Paolino data (grey line). The thick black line in (b) represents the 20-year low-pass filtered Δ SLP and the red dotted line indicates the Δ SLP trend as that shown in Panagiotopoulos *et al.* (2005). The time period between 1976 and 2001 where the great SH decline was noted is shaded in light yellow. This figure is available in colour online at wileyonlinelibrary.com/journal/joc

System. Given the difference of time periods between ERA40 (1958–2001) and ERA-Interim (1989–present), these two reanalyses are combined and evaluated as one, denoted as ERA40/I. This is done by averaging the two over their overlapping time period (1989–2001). For observations, we use two gridded SLP data, one generated by Trenberth and Paolino (1980) and the other by the UK Met Office Hadley Centre (HadSLP2; Allan and Ansell, 2006). Daily maximum and minimum temperatures and surface pressure at three stations [Wuhan (WMO ID: 57494), Taipei (46692), and Hong Kong (45005), locations shown in Figure 1(a)] that have been used to study cold surges (Wu and Chan, 1995; Chen *et al.*, 2002; Wu and Leung, 2008) are also analysed. In the reanalyses, the ‘station’ temperature and SLP are obtained through linear interpolation from the four grid points surrounding each station. A bias correction is then applied by removing the differences in seasonal mean between the reanalyses and the station records. The analysis period covers the winter season (December–February) from 1950 to 2008.

Following Panagiotopoulos *et al.* (2005), the SH intensity is determined by SLP averaged over the SH domain (Figure 1(a)). The occurrence of a cold surge is defined by the following criteria: (1) the SLP averaged over the SH must be >1035 hPa, (2) the surface temperature (i.e. the average of daily maximum and minimum temperature) at each station experiences a decrease of at least 4 °C within 24 h, and (3) the daily minimum temperature at each station is <15 °C on or after the day of temperature decrease. These criteria are modified from Zhang *et al.* (1997) with additional minimum temperature conditions at the surface stations (i.e. the third criterion), following Hong *et al.* (2008). The observed cold surge frequencies in Wuhan, Taipei, and Hong Kong from 1950 to 2008 are shown in Figure 2(c)–(e). The average number of cold surges at these three stations is about 13 cases per winter

in the 1976–1987 period and 11 cases in 1988–2001, close to the numbers found in Zhang *et al.* (1997).

Zhang *et al.* (1997) required surface air temperature to drop 8–10 °C in central China or 5–7 °C in southern China within 24–48 h of the onset of the cold surge. We require a temperature drop of at least 4 °C in the southeast stations but add a criterion of daily minimum temperature <15 °C in order to filter out the weaker surges. Focusing on stronger cold surges helps to evaluate the performance of global reanalyses on depicting cold surges. Without the criterion of daily minimum temperature <15 °C, the average number of cold surges in Figure 2(c)–(e) would be about 35% higher approaching those shown in Chen *et al.*, 2004 (17.3 cases per year). However, Jeong and Ho (2005) applied different criteria (i.e. surface air temperature decrease >2 standard deviations and anomalous northerly wind speed >1.5 standard deviations) in addition to Zhang *et al.*'s (1997) criteria. This may be why Jeong and Ho's (2005) number of cold surges (8.39 cases per winter) is smaller than Zhang *et al.*'s and ours.

3. Results

3.1. Siberian high

The SH intensity in the various reanalysis data sets is shown by the SLP time series in Figure 2(a). All data sets agree well with each other in terms of the interannual variability. As shown in Table II, the correlation coefficients between the Trenberth–Paolino data and other data sets are significantly high. To depict the interdecadal variability, the SLP time series are smoothed by a 20-year low-pass filter with the minimum slope constraint following Mann (2004). This low-pass method gives the least spurious trends on both ends of the time series. After filtering, the late 20th century decline of the SH in the

Table I. List of observations and reanalysis data sets.

Name	Period	Model resolution	Interpolation or assimilation scheme	Reference and DS home page address
WMO surface stations	1950–present	–	–	http://dss.ucar.edu/datasets/ds564.0/
National Center for Atmospheric Research (NCAR) (Trenberth and Paolino) Northern Hemisphere SLP (herein Trenberth–Paolino data)	1899–April 2009	–	–	Trenberth and Paolino (1980) http://dss.ucar.edu/datasets/ds010.1/
The Met Office Hadley Centre's mean sea-level pressure data set (herein HadSLP2)	1850–2004	–	–	Allan and Ansell (2006) http://dss.ucar.edu/datasets/ds277.4/
National Centers for Environmental Prediction (NCEP)–NCAR Re-Analysis (herein NCEP1)	1948–present	T62 L28	Reduced-space optimal interpolation	Kalnay <i>et al.</i> (1996) http://dss.ucar.edu/datasets/ds090.0/
NCEP–Department of Energy Atmospheric Model Intercomparison Project (AMIP-II) Re-Analysis (herein NCEP2)	1979–present	T62 L28	3DVAR	Kanamitsu <i>et al.</i> (2002) http://dss.ucar.edu/datasets/ds091.0/
The European Centre for Medium-Range Weather Forecasts (ECMWF) Re-Analysis (herein ERA40)	September 1957–August 2002	T159 L60	3DVAR	Uppala <i>et al.</i> (2005) http://dss.ucar.edu/datasets/ds120.0/
The ECMWF Interim Re-Analysis (herein ERA-interim)	1989–present	T255 L60	3DVAR	Simmons <i>et al.</i> (2007) http://dss.ucar.edu/datasets/ds627.0/
Japanese 25-year Reanalysis Project (herein JRA25)	1979–present	T106 L40	4DVAR	Onogi <i>et al.</i> (2007) http://dss.ucar.edu/datasets/ds625.1/
Goddard Earth Observing System Data Assimilation System Version 5 (herein GEOS5)	1979–August 2006	L72	3DVAR	http://gmao.gsfc.nasa.gov/pubs/docs/GEOS5_104606-Vol27.pdf

T, triangular truncation; L, vertical layers.

Trenberth–Paolino data is considerably deeper than that in all other data sets, including HadSLP2 (Figure 2(b)). Except NCEP2, all data sets depict a similar phase of the interdecadal variation during the 1976–2001 period, although the magnitude of the variation in the Trenberth–Paolino data is notably larger than the others.

Before 1979, there is a substantial difference between NCEP1 and ERA40/I and between these two reanalyses and the observations (Figure 2(b)). After 1979, all the reanalyses become increasingly consistent with one another and with HadSLP2, but none of them depicts the SH decline as dramatic as that shown in Panagiotopoulos *et al.* (2005) with the Trenberth–Paolino data. Such an inconsistency is reflected by the relatively low correlation coefficients between the Trenberth–Paolino data and other data sets in the interdecadal time scale compared to the interannual time scale (Table II). In 1979, a global observing system was established during the Global Weather Experiment with the implementation of a comprehensive space-borne observing system. It is plausible that the inclusion of the global observational records beginning from 1979 resulted in considerable differences between surface station-based and assimilation data sets. From Figure 2(a) it is also

visible that the SH trend levels off in 1993 in all data sets except the Trenberth–Paolino data. The timing of the difference coincides with the 1994 launch of the second-generation Geostationary Operational Environmental Satellites replacing the first-generation ones that covered 1980–1993. How the upgraded satellite data contributed to such an inconsistency in the post-1993 SH variation is unclear. However, we note that all reanalyses agree well with the HadSLP2, signalling that even different observational data sets can yield different results regarding the SH variability.

Possible causes for the discrepancy in trends between reanalyses have been discussed by a number of studies (Sturaro, 2003; Sterl, 2004; Salstein *et al.*, 2008). Because reanalyses are naturally sensitive to historical changes in the observing system (such as the establishments of global radiosonde network in 1958 and satellite observations thriving since the 1970s), different assimilation schemes between reanalyses could lead to large discrepancies in temporal variations (Bengtsson *et al.*, 2004; Bromwich and Fogt, 2004). For example, NCEP1 only assimilates retrieved atmospheric temperature profiles, while ERA40 includes satellite observations (Cai and Kalnay, 2005; Chen *et al.*, 2008). Furthermore,

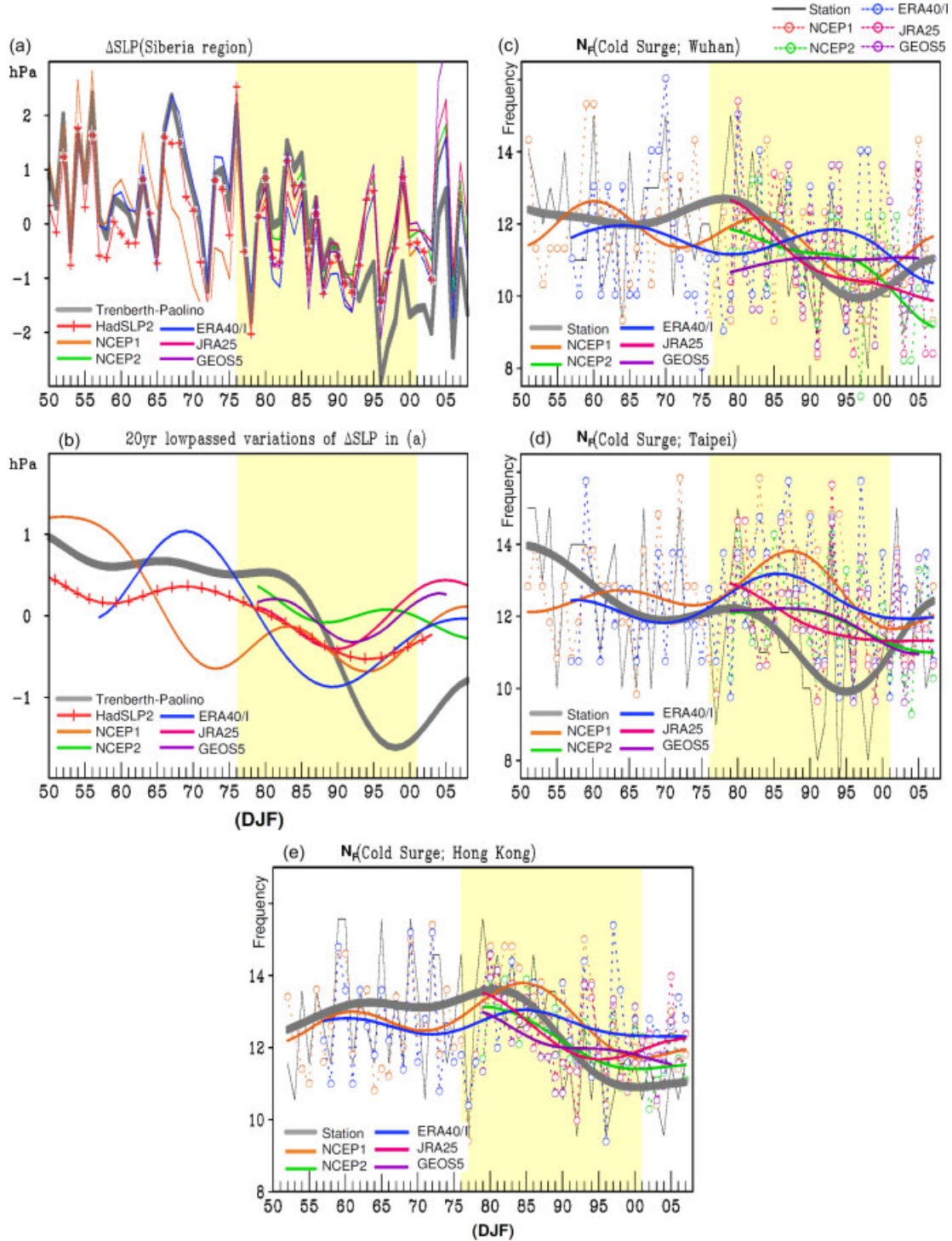


Figure 2. (a) Same as Figure 1(b) but for the total variations of observed ΔSLP (Trenberth–Paolino data and HadSLP2) and assimilated ΔSLP (NCEP1, NCEP2, ERA40/I, JRA25, and GEOS5). (b) The 20-year lowpassed variations of (a). (c)–(e) The wintertime cold surge frequencies (N_F) in Wuhan, Taipei, and Hong Kong observed from stations and the reanalyses. Solid thin lines (dotted thin lines with open circles) show the actual time series of observed (assimilated) N_F and solid thick lines are the associated 20-year lowpassed variations. The legend is shown in the lower left in (a)–(e) and atop (c). The time period between 1976 and 2001 where the great SH decline was noted is shaded in light yellow.

This figure is available in colour online at wileyonlinelibrary.com/journal/joc

because NCEP1 was conducted earlier than ERA40, newer observations were purposely excluded in NCEP1 in order to maintain a stable output over time (Sterl, 2004). This might have led to the sudden increase of discrepancies in various fields during the late 1960s between ERA40 and NCEP1. Moreover, as the assimilated surface

pressure is linked to the total mass of the atmosphere, errors from any factors affecting the total mass of the atmosphere would likely contribute to the trend of SH and, in turn, affect the trend of cold surge frequencies. For example, NCEP1 only has water vapour data input from radiosonde observations, whereas water vapour retrieved

Table II. Correlation coefficient (r) between reanalysis and observation for the SLP over Siberia and the cold surge frequencies in southeast stations during 1950–2008.

	HadSLP2	NCEP1	NCEP2	ERA40/I	JRA25	GEOS5
Interannual time scale						
$r[\text{SH}(\text{reanalysis} \times \text{observation})]$	0.96	0.92	0.97	0.96	0.95	0.95
$r[S_g(\text{reanalysis} \times \text{observation})]$ Wuhan	–	0.34	0.35	0.24	0.46	0.22
$r[S_g(\text{reanalysis} \times \text{observation})]$ Taipei	–	0.30	0.34	0.22	0.64	0.43
$r[S_g(\text{reanalysis} \times \text{observation})]$ Hong Kong	–	0.45	0.42	0.46	0.24	0.14
Interdecadal time scale						
$r[\text{SH}(\text{reanalysis} \times \text{observation})]$	0.73	0.30	0.25	0.35	–0.23	0.20
$r[S_g(\text{reanalysis} \times \text{observation})]$ Wuhan	–	0.47	0.20	–0.18	0.40	–0.11
$r[S_g(\text{reanalysis} \times \text{observation})]$ Taipei	–	–0.21	–0.19	–0.13	0.30	0.05
$r[S_g(\text{reanalysis} \times \text{observation})]$ Hong Kong	–	0.70	0.82	0.28	0.35	0.24

SH, sea-level pressure over Siberia region; S_g , cold surge. Interdecadal time scale: 20-year low-pass filtered values in Figure 2. Correlation coefficient above 95% confidence interval is emphasised with bold type.

from satellite data is assimilated in ERA40 after 1987, suggesting that more water vapour is included in ERA40 than in NCEP1 (Chen *et al.*, 2008).

3.2. Cold surge frequencies

Next, we evaluate the representation of cold surge frequencies from the six reanalyses. Cold surge frequencies in Wuhan, Taipei, and Hong Kong constructed from reanalyses are shown, respectively, in Figure 2(c)–(e), following Figure 2(a)–(b). It is evident that the cold surge frequency at the three stations (grey line in Figure 2(c)–(e)) decreases considerably during the 1976–2001 period and then increases afterward, except in Hong Kong where cold surges remain less active throughout the 21st century, as was noted in Wu and Leung (2008). Such low-frequency variations in the cold surge frequency are highly correlated with the SH variation (grey line in Figure 2(b)), particularly in Wuhan and Hong Kong where ocean modification of cold surges is minimal. Similar interdecadal correspondence between cold surges and the SH has also been noted in Taiwan by Hong *et al.* (2008) based on surface observations.

As shown in Table II, the interannual variations of cold surge frequencies are positively correlated with the observations, although the correlation is not as high as that of the SH variations. This may reflect a limitation of the coarse-resolution reanalyses in replicating station records based on which the cold surge criteria are defined. In the interdecadal time scale (i.e. filtered by the 20-year lowpass), the coherence between cold surge frequencies in reanalyses and observation remains weak (Figure 2(c)–(e) and Table II). For example, at Wuhan only NCEP1 and JRA25 give a trend in the post-1980 cold surge frequency similar to that in the observations, albeit weak. The interdecadal variation in ERA40/I and GEOS5 is nearly opposite to the observation (Figure 2(c)). In Taipei, the disagreement among data sets is more serious; only JRA25 depicts a coherent but much weaker trend (Figure 2(d)). In Hong Kong, however, JRA25, NCEP1, and NCEP2 show relatively consistent trends in the cold surge frequency with

the observations (Figure 2(e)). Table II summarises the correlation coefficients between reanalyses and observations which support the analysis made in Figure 2.

The reanalyses that are more consistent with the observations in cold surges do not necessarily depict the SH trend better (e.g. NCEP1). Some reanalyses (GEOS5 and ERA40/I) even reveal opposite decadal variations between the SH and the cold surge frequency. Because surface air temperature change in southeast stations is one of the criteria for cold surge identification (i.e. Section 2), the inconsistency between the trend of SH and cold surge frequency in Figure 2 leads to a speculation that reanalyses, which do not represent the SH trend well, may handle surface air temperature in southeast stations differently. Visual inspection of the trend and variability of surface air temperature in Wuhan, Taipei, and Hong Kong (Figure 3(a)–(c)) suggests that, after 1960, all six reanalyses are in good agreement with the station records. In contrast, substantial differences between reanalyses and observations are found over Siberia (Figure 3(d)). Examinations of correlation coefficients (Table III) between the observed surface air temperature and other data sets from Figure 3 indicate that the correlation is consistently lower over Siberia than that in southern Asia, even though the correlation remains significant in all areas (except GEOS5). This contrast between the correlations over Siberia and southeast stations (Table III) suggests that reanalyses represent the surface air temperature better in Southeast Asia than Siberia.

To further explain the geographic difference of trends in both SLP and surface air temperature between reanalyses and observations, we examine the horizontal distributions of the difference of SLP (i.e. ΔSLP ; contours in Figure (4)) and surface air temperature (i.e. ΔT_s ; shadings in Figure (4)) between the 1979–1993 and 1994–2009 periods. The selection of these two time periods is based on the fact that the SH trend levels off in 1993 in most data sets except the Trenberth–Paolino data (Figure 2(a)). It appears that the magnitudes of ΔSLP between observation and other data sets are larger over Siberia than Southeast Asia. A clear

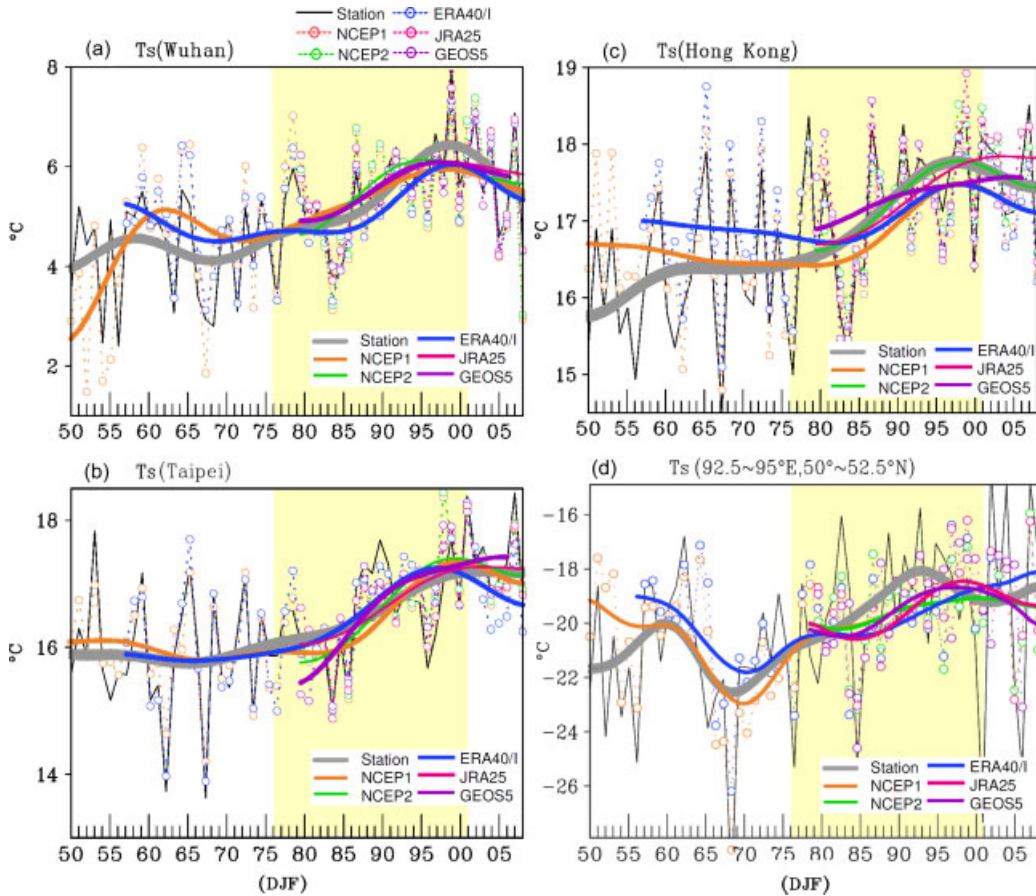


Figure 3. The times series of DJF-averaged temperature in (a) Wuhan, (b) Taipei, and (c) Hong Kong obtained from surface stations (solid thin line) and the reanalyses (dotted thin lines with open circles). The 20-year lowpass filtered temperatures are added in (a)–(c) by thick solid lines with the corresponding colour. (d) Similar to (a)–(c), but for DJF-averaged temperature area-averaged over 92.5° – 95° E, 50° – 52.5° N (located by a blue open triangle in Figure 4; a centre over Siberia with largest decline of SLP trend). The legend for those thick lines and thin lines is given in the lower right in (a)–(d) and atop (a). The time period between 1976 and 2001 where the great SH decline was noted is shaded in light yellow. This figure is available in colour online at wileyonlinelibrary.com/journal/joc

anomalous low of Δ SLP located over Siberia is revealed in the Trenberth–Paolino data (Figure 4(a)), but none of the reanalyses (Figure 4(b)–(f)) depicts this anomalous low with the same intensity. Previous studies (Yang *et al.*, 2002; Inoue and Matsumoto, 2004) have also

noted a similar discrepancy of SLP of NCEP1 in the region.

It is also revealed in Figure 4 that the magnitude of surface air temperature warming is larger in northern China than Southeast Asia (Wang and Gaffen, 2001). Over

Table III. Correlation coefficient (r) between reanalysis and observation for the surface air temperature in southeast stations and Siberia during 1950–2008.

	NCEP1	NCEP2	ERA40/I	JRA25	GEOS5
Interannual time scale					
$r[T_s(\text{reanalysis} \times \text{observation})]$ Wuhan	0.76	0.84	0.93	0.96	0.94
$r[T_s(\text{reanalysis} \times \text{observation})]$ Taipei	0.90	0.85	0.88	0.91	0.82
$r[T_s(\text{reanalysis} \times \text{observation})]$ Hong Kong	0.86	0.89	0.73	0.90	0.88
$r[\Delta T_s(\text{reanalysis} \times \text{observation})]$ (92.5° – 95° E, 50° – 52.5° N)	0.63	0.54	0.55	0.49	0.35
Interdecadal time scale					
$r[T_s(\text{reanalysis} \times \text{observation})]$ Wuhan	0.79	0.89	0.93	0.95	0.97
$r[T_s(\text{reanalysis} \times \text{observation})]$ Taipei	0.95	0.98	0.94	0.99	0.96
$r[T_s(\text{reanalysis} \times \text{observation})]$ Hong Kong	0.84	0.99	0.83	0.90	0.80
$r[\Delta T_s(\text{reanalysis} \times \text{observation})]$ (92.5° – 95° E, 50° – 52.5° N)	0.69	0.63	0.56	0.53	0.48

T_s , surface air temperature; Interdecadal time scale: 20-year low-pass filtered values in Figure 3. Correlation coefficient above 0.7 is emphasised with bold type.

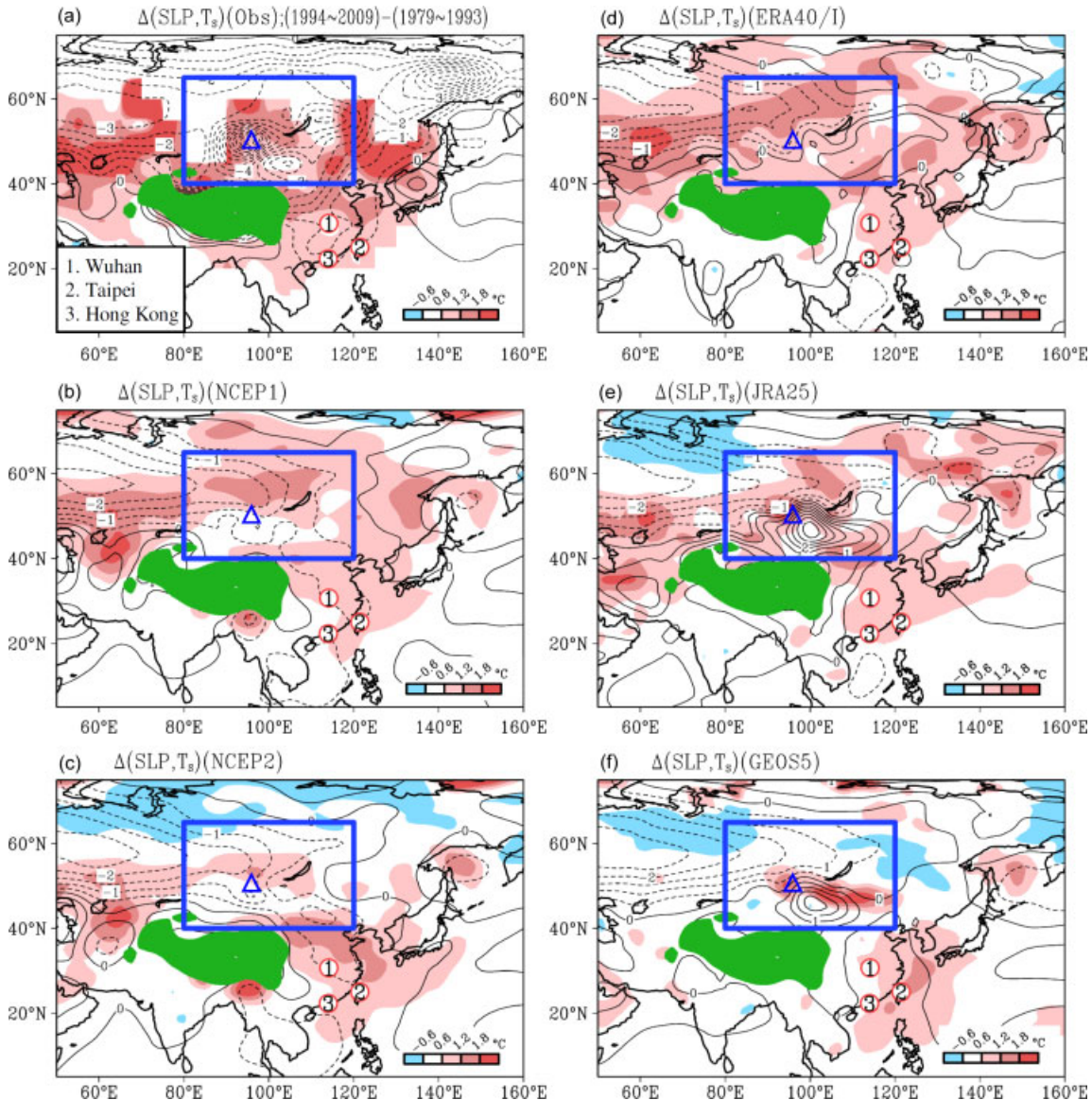


Figure 4. Decadal change of DJF averaged [SLP (contour), T_s (shading)] between the time periods of 1979–1993 and 1994–2009 for observation and reanalyses. The colour scale of ΔT_s is given in the right bottom. The contour interval of ΔSLP is 0.5 hPa. The location of Wuhan, Taipei, and Hong Kong is denoted by a red open circle in (a)–(f). The location of blue open triangle within Siberia (blue boxed area) is selected for the analysis of Figure 3(d). This figure is available in colour online at wileyonlinelibrary.com/journal/joc

Siberia, ΔT_s also exhibits pronounced spatial differences between observation and reanalyses, but the differences are not as significant as those revealed in ΔSLP (Figure 4). This explains why the correlation coefficients between observation and reanalyses are lower for the SH trend (seventh row in Table II) than the T_s trend over Siberia (tenth row in Table III). As for the spatial variation of SLP and T_s trends in Southeast Asia shown in Figure 4, the differences between observation and reanalyses are not as significant as those revealed over Siberia.

It is noted that in the inner parts of China such as Wuhan (Figure 3(a)), surface air temperature in the earlier period of NCEP1 (before 1960) does not correspond well with the observation, possibly due to insufficient early observations. Also noteworthy is the widespread warming in all data sets accompanied by intensified warming corresponding to the SH declining

period (1978–2001). The warming levelled off at the end of the 20th century and began to cool from 2000 onward. Such temperature characteristics are consistent with those observed worldwide (Knight *et al.*, 2009). More importantly, the consistency in surface temperature speaks for the capability of reanalyses in replicating surface features over Southeast Asia, despite their general disagreements in the variations of the SH and Southeast Asian cold surge frequency. The documented discrepancies ought to be taken into account in future research for the EAWM interdecadal variability.

4. Summary

Over the past half century, both the SH and the cold surge frequency have undergone pronounced interdecadal

variations. Analysing six modern reanalyses and observations, this study reports apparent discrepancies in such interdecadal variations. The rapid decline of the SH as noted in Panagiotopoulos *et al.* (2005) is found to be considerably less pronounced in all six reanalyses. The associated decrease in the cold surge frequency recorded from stations is also consistently weaker in reanalyses. However, the interannual variations of both the SH and cold surges are fairly consistent between reanalyses and observations, suggesting that changes in the assimilation process of individual reanalyses may be a factor. In addition, changes in the observing system are also possible to cause the different trends of SH and cold surge frequency between reanalyses.

The interdecadal variation of surface variables in the longer-term reanalyses (i.e. NCEP1 and ERA40/I) appears to exhibit more uncertainty in inland China (i.e. Wuhan) than the southern coast (i.e. Hong Kong) and in Siberia than Southeast Asia. This is likely due to the complication of surface/terrain effect as well as data quality, as Hong Kong has a much longer and complete record than most of the stations in China. The actual cause for such discrepancy among reanalyses remains an open question. Nevertheless, the documented inconsistency of reanalyses in the depiction of the SH and cold surges can cause misinterpretation of the EAWM variability when using these reanalyses and, therefore, deserves attention.

Acknowledgements

We thank two anonymous reviewers for their comments and suggestions which greatly improved this study. SYW is supported by the USDA-CSREES funded Drought Management, Utah Project.

References

- Allan R, Ansell T. 2006. A new globally complete monthly historical gridded mean sea level pressure dataset (HadSLP2): 1850–2004. *Journal of Climate* **19**: 5816–5842.
- Bengtsson L, Hagemann S, Hodges KI. 2004. Can climate trends be calculated from reanalysis data? *Geophysical Research Letters* **109**: D11111, DOI:10.1029/2004JD004536.
- Bromwich DH, Fogt RL. 2004. Strong trends in the skill of the ERA-40 and NCEP–NCAR reanalyses in the high and midlatitudes of the Southern Hemisphere, 1958–2001. *Journal of Climate* **17**: 4603–4619.
- Cai M, Kalnay E. 2005. Can reanalysis have anthropogenic climate trends without model forcing? *Journal of Climate* **18**: 1844–1849.
- Chan J, Li C. 2004. East Asia winter monsoon. In *East Asian Monsoon*, Chang CP (ed). World Scientific Series on Meteorology of East Asia. World Scientific Publication: Singapore; Vol. 2; 54–106.
- Cheang BK. 1987. Short- and long-range monsoon prediction in Southeast Asia. In *Monsoons*, Fein JS, Stephens PL (eds). John Wiley & Sons: New York; 579–606.
- Chen W, Graf HF, Huang RH. 2001. The interannual variability of East Asian winter monsoon and its relation to the summer monsoon. *Advances in Atmospheric Sciences* **17**: 48–60.
- Chen TC, Yen MC, Huang WR, Gallus WA. 2002. An East Asian cold surge: case study. *Monthly Weather Review* **130**: 2271–2290.
- Chen TC, Huang WR, Yoon JH. 2004. Interannual variation of the East Asian cold surge activity. *Journal of Climate* **17**: 401–413.
- Chen J, Genio ADD, Carlson BE, Bosilovich MG. 2008. The spatiotemporal structure of twentieth-century climate variations in observations and reanalyses. Part II: Pacific pan-decadal variability. *Journal of Climate* **21**: 2634–2650.
- Ding YH. 1990. Build-up, air mass transformation and propagation of Siberian high and its relation to cold surge in East Asia. *Meteorology and Atmospheric Physics* **44**: 281–292.
- Gao H. 2007. Comparison of East Asian winter monsoon indices. *Advanced Geosciences* **10**: 31–37.
- Gong DY, Ho CH. 2002. The Siberian High and climate change over middle to high latitude Asia. *Theoretical and Applied Climatology* **72**: 1–9.
- Greatbatch RJ, Rong PP. 2006. Discrepancies between different northern hemisphere summer atmospheric data products. *Journal of Climate* **19**(7): 1261–1273.
- Hong CC, Hsu HH, Chia HH, Wu CY. 2008. Decadal relationship between the North Atlantic Oscillation and cold surge frequency in Taiwan. *Geophysical Research Letters* **35**: L24707, DOI:10.1029/2008GL034766.
- Inoue T, Matsumoto J. 2004. A comparison of summer sea level pressure over east Eurasia between NCEP–NCAR reanalysis and ERA-40 for the period 1960–99. *Journal of the Meteorological Society of Japan* **82**: 951–958.
- Jeong JH, Ho CH. 2005. Changes in occurrence of cold surges over east Asia in association with Arctic oscillation. *Geophysical Research Letters* **32**: L14704, DOI:10.1029/2005GL023024.
- Jhun JG, Lee EJ. 2004. A new East Asian winter monsoon index and associated characteristics of the winter monsoon. *Journal of Climate* **17**: 711–726.
- Kalnay E, Kanamitsu M, Kistler R, Collins W, Deaven D, Gandin L, Iredell M, Saha S, White G, Woollen J, Zhu Y, Leetmaa A, Reynolds R, Chelliah M, Ebisuzaki W, Higgins W, Janowiak J, Mo K, Ropelewski C, Wang J, Jenne R, Joseph D. 1996. The NCEP/NCAR 40-year reanalysis project. *Bulletin of the American Meteorological Society* **77**: 437–471.
- Kanamitsu M, Ebisuzaki W, Woollen J, Yang SK, Hnilo JJ, Fiorino M, Potter GL. 2002. NCEP–DOE AMIP-II reanalysis (R-2). *Bulletin of the American Meteorological Society* **83**: 1631–1643.
- Knight J, Kennedy JJ, Folland C, Harris G, Jones GS, Palmer M, Parker D, Scaife A, Stott P. 2009. Do global temperature trends over the last decade falsify climate predictions? [in “State of the Climate in 2008”]. *Bulletin of the American Meteorological Society* **90**: 22–23.
- Lau KM, Chang CP. 1987. Planetary scale aspects of winter monsoon and teleconnections. In *Monsoon Meteorology*, Chang CP, Krishnamurti TN (eds). Oxford University Press: Oxford; 161–202.
- Lim HS, Ho CH. 2000. Comparison of observed precipitation of GPCP with assimilated precipitation from ECMWF, NCEP/NCAR, and NASA/GEOS-1 reanalyses. *Journal of Meteorological Society in Japan* **78**: 661–672.
- Mann ME. 2004. On smoothing potentially non-stationary climate time series. *Geophysical Research Letters* **31**: L07214, DOI:10.1029/2004GL019569.
- Onogi K, Tsutsumi J, Koide H, Sakamoto M, Kobayashi S, Hatushika H, Matsumoto T, Yamazaki N, Kamahori H, Takahashi K, Kadokura S, Wada K, Kato K, Oyama R, Ose T, Mannoji N, Taira R. 2007. The JRA-25 reanalysis. *Journal of the Meteorological Society of Japan* **85**: 369–432.
- Panagiotopoulos F, Shahgedanova M, Hannachi A, Stephenson DB. 2005. Observed trends and teleconnections of the Siberian high: a recently declining center of action. *Journal of Climate* **18**: 1411–1422.
- Ponte RM, Dorandeu J. 2003. Uncertainties in ECMWF surface pressure fields over the ocean in relation to sea level analysis and modeling. *Journal of Atmospheric and Oceanic Technology* **20**: 301–307.
- Salstein DA, Ponte RM, Pereira KC. 2008. Uncertainties in atmospheric surface pressure fields from global analyses. *Journal of Geophysical Research* **113**: D14107, DOI:10.1029/2007JD009531.
- Shi N. 1996. Features of the East Asian winter monsoon intensity on multiple time scale in recent 40 years and their relation to climate. *Journal of Applied Meteorological Sciences* **7**: 175–182.
- Simmons A, Uppala S, Dee D, Kobayashi S. 2007. ERA-Interim: new ECMWF reanalysis products from 1989 onwards. Newsletter 110 – Winter 2006/07, ECMWF; 11 pp.
- Smith SR, Legler DM, Verzone KV. 2001. Quantifying uncertainties in NCEP reanalyses using high-quality research vessel observations. *Journal of Climate* **14**: 4062–4072.
- Sterl A. 2004. On the (in)homogeneity of reanalysis products. *Journal of Climate* **17**: 3866–3873.

- Sturaro G. 2003. A closer look at the climatological discontinuities present in the NCEP–NCAR reanalysis temperature due to the introduction of satellite data. *Climate Dynamics* **21**: 309–316.
- Suman N, Alfredo RB. 2006. Seasonal hydroclimate variability over north America in global and regional reanalysis and AMIP simulations: varied representation. *Journal of Climate* **19**(5): 815–837.
- Sun SQ, Sun BM. 1995. The relationship between the anomalous winter monsoon circulation over East Asia and summer drought/flooding in the Yangtze and Huaihe River valley. *Acta Meteorological Sinica* **57**: 513–522.
- Trenberth KE, Paolino DA Jr. 1980. The Northern Hemisphere sea-level pressure data set: trends, errors and discontinuities. *Monthly Weather Review* **108**: 855–872.
- Uppala SM, Allberg K, Simmons PW, Andrae AJ, Da Costa U, Bechtold V, Fiorino M, Gibson JK, Haseler J, Hernandez A, Kelly GA, Li X, Onogi K, Saarinen S, Sokka N, Allan RP, Andersson E, Arpe K, Balmaseda MA, Beljaars ACM, Van De Berg L, Bidlot J, Bormann N, Caires S, Chevallier F, Dethof A, Dragosavac M, Fisher M, Fuentes M, Hagemann S, H'olm E, Hoskins BJ, Isaksen L, Janssen PAEM, Jenne R, McNally AP, Mahfouf J-F, Morcrette J-J, Rayner NA, Saunders RW, Simon P, Sterl A, Trenberth KE, Untch A, Vasiljevic D, Viterbo P, Woollen J. 2005. The ERA-40 re-analysis. The ERA-40 re-analysis. *Quarterly Journal of the Royal Meteorological Society* **131**: 2961–3012.
- Wang XL, Gaffen DJ. 2001. Late twentieth century climatology and trends of surface humidity and temperature in China. *Journal of Climate* **14**: 2833–2845.
- Wu MC, Chan JCL. 1995. Surface features of winter monsoon surges over South China. *Monthly Weather Review* **123**: 662–680.
- Wu MC, Chan JCL. 1997. Upper-level features associated with winter monsoon surges over South China. *Monthly Weather Review* **125**: 317–340.
- Wu MC, Leung WH. 2008. Effect of ENSO on winter monsoon affecting Hong Kong. HKO Reprint No. 789.
- Wu B, Wang J. 2002. Winter Arctic oscillation, Siberian high and East Asian winter monsoon. *Geophysical Research Letters* **29**: 1897–1901, DOI:10.1029/2002GL015373.
- Yang S, Lau KM, Kim KM. 2002. Variations of the East Asian jet stream and Asian–Pacific–American winter climate anomalies. *Journal of Climate* **15**: 306–325.
- Zhao TB, Fu CB. 2006. Comparison of products from ERA-40, NCEP-2, and CRU with station data for summer precipitation over China. *Advances in Atmospheric Sciences* **23**: 593–604, DOI:10.1007/s00376-006-0593-1.
- Zhang Y, Sperber KR, Boyle JS. 1997. Climatology and interannual variation of the East Asian winter monsoon: results from the 1979–95 NCEP/NCAR reanalysis. *Monthly Weather Review* **125**: 2605–2619.